Tetrahedron 75 (2019) 1711–1716

Contents lists available at ScienceDirect

Tetrahedron

journal homepage: www.elsevier.com/locate/tet

Alkaloids from the roots of *Stemona tuberosa* and their anti-tobacco mosaic virus activities

Zhan-Xing Hu [a, b, c, d, e, 1], Hong-Yu Tang [a, f, 1], Jie Guo [a], Haji Aker Aisa [b], Yu Zhang [a, *], Xiao-Jiang Hao [a, d, e, **]

[a] State Key Laboratory of Phytochemistry and Plant Resources in West China, Kunming Institute of Botany, Chinese Academy of Sciences, Kunming 650201, PR China
[b] The Xinjiang Technical Institute of Physics & Chemistry, Chinese Academy of Sciences, Urumqi 830011, PR China
[c] University of Chinese Academy of Sciences, Yuquan Road 19, Beijing 100049, PR China
[d] State Key Laboratory of Functions and Applications of Medicinal Plants, Guizhou Medical University, Guiyang 550014, PR China
[e] The Key Laboratory of Chemistry for Natural Products of Guizhou Province and Chinese Academy of Sciences, Guiyang 550002, PR China
[f] School of Chemical Science and Technology, Yunnan University, Kunming 650091, PR China

A R T I C L E I N F O

Article history:
Received 10 October 2018
Received in revised form
28 November 2018
Accepted 29 November 2018
Available online 5 December 2018

Keywords:
Stemona tuberosa
Stemona alkaloids
Stemtuberline A
Anti-TMV

A B S T R A C T

Stemtuberlines A (**1**) and B (**2**), two new alkaloids with a unique tricyclic pyrrolo [3,2,1-*jk*]benzazepine-12-one nucleus, three new croomine-type alkaloids, stemtuberlines C-E (**3**–**5**), together with seven known ones were isolated from the roots of *Stemona tuberosa*. The structures of the new alkaloids were elucidated based on a comprehensive spectroscopic data analysis. The absolute configurations of **1** and **2** were determined by quantum ECD calculations. The anti-tobacco mosaic virus activity of the *Stemona* alkaloids was firstly evaluated and compound **11** exhibited significant anti-tobacco mosaic virus activity with the curative inhibition rate of 84.6% at concentration of 50 μg/mL.

© 2018 Elsevier Ltd. All rights reserved.

1. Introduction

Stemonaceae is a small monocotyledonous family comprising three genera, *Stemona*, *Croomia*, and *Stichoneuron* [1]. The genus *Stemona* is well known for containing structurally unique stemona alkaloids characterized by the presence of the pyrrolo [1,2-*a*]azepine nucleus. Up to now, more than 150 alkaloids have been isolated from this genus [2]. Some of these alkaloids were found to exhibit various bioactivities including insect toxicity, antifeedant, nematicidal activity, repellent activity, and antitussive activity [3]. The structural diversity and the potential biological significance of these alkaloids motivated us to conduct a further investigation on the genus *Stemona* plants. As part of this research program, the chemical constituents of the roots of *Stemona tuberosa* were investigated, which resulted in the isolation of two new stemona alkaloids, stemtuberlines A (**1**) and B (**2**), three new croomine-type alkaloids (**3**–**5**), along with seven known ones (**6**–**12**). It is noteworthy that alkaloids **1** and **2** represent the first examples of stemona alkaloids with an unusual tricyclic pyrrolo [3,2,1-*jk*] benzazepine-12-one nucleus within stemona alkaloids category (Fig. 1). In addition, the *anti*-TMV activity of the isolates were firstly evaluated and the results revealed that compound **11** exhibited significant *anti*-TMV activity with the curative inhibition rate of 84.6% at concentration of 50 μg/mL. Herein, we report the isolation, structure elucidation and biological tests of these alkaloids.

2. Results and discussion

2.1. Structure elucidation of the compounds

Stemtuberline A (**1**) was obtained as a white solid, and its molecular formula was assigned as $C_{18}H_{25}NO_3$, with seven degrees of

* Corresponding author. State Key Laboratory of Phytochemistry and Plant Resources in West China, Kunming Institute of Botany, Chinese Academy of Sciences, Kunming 650201, PR China.
** Corresponding author. State Key Laboratory of Phytochemistry and Plant Resources in West China, Kunming Institute of Botany, Chinese Academy of Sciences, Kunming 650201, PR China.
E-mail addresses: zhangyu@mail.kib.ac.cn (Y. Zhang), haoxj@mail.kib.ac.cn (X.-J. Hao).
[1] The first two authors contributed equally to this work.

https://doi.org/10.1016/j.tet.2018.11.064
0040-4020/© 2018 Elsevier Ltd. All rights reserved.

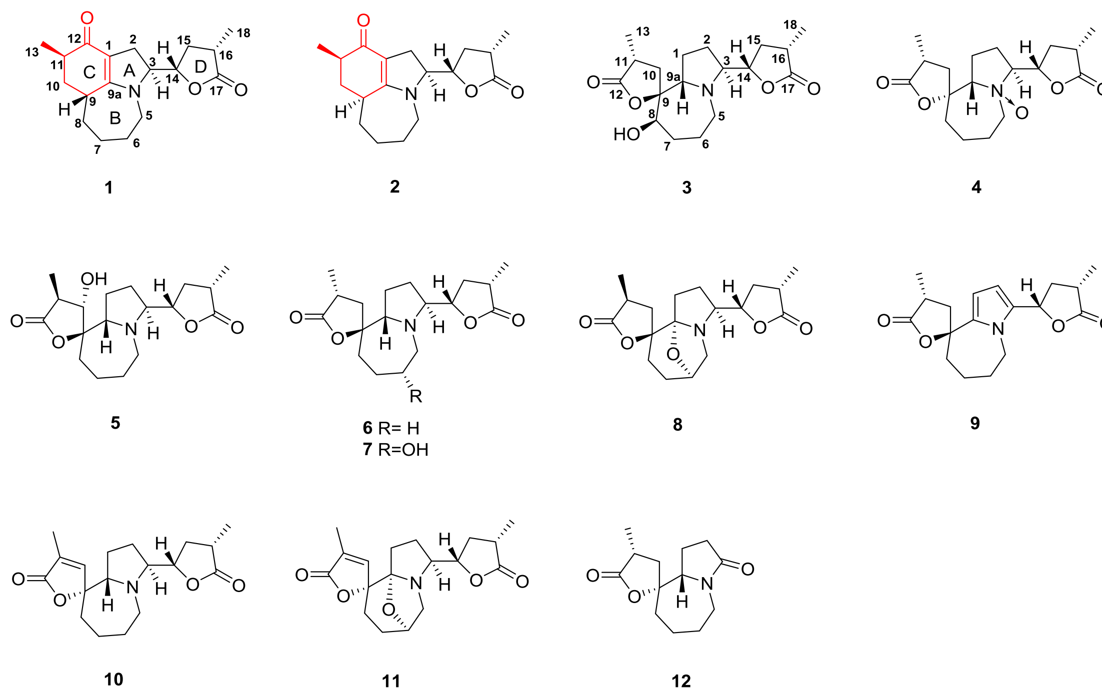

Fig. 1. Structures of compounds **1**–**12**.

unsaturation, from its HRESIMS (m/z 326.1724 [M + Na]$^+$, calcd for 326.1727) and NMR data (Tables 1 and 2). The IR spectrum clearly exhibited absorption bands of ketone or ester carbonyl (1768, 1717 cm^{-1}) functionalities. The ^{1}H and ^{13}C NMR spectra (Tables 1 and 2) showed the signals of two methyls (δ_C 16.3, δ_H 1.03, d, J = 7.0 Hz; δ_C 15.0, δ_H 1.22 d, J = 7.0 Hz), one nitrogenated methylene (δ_C 48.4, δ_H 3.69, dd, J = 15.4, 5.8 Hz; δ_H 3.44, dd, J = 15.4, 11.3 Hz), and two heteroatom-substituted methines (δ_C 81.5, δ_H 4.45, 1H, ddd, J = 10.8, 8.4, 5.5 Hz; δ_C 68.7, δ_H 3.94, 1H, dt, J = 11.0, 8.3 Hz). The ^{13}C and DEPT NMR spectra displayed resonances for two methyls, seven methylenes, five methines, and four quaternary carbons (Table 2). The aforementioned evidence suggested that compound

Table 1
^{1}H NMR spectroscopic data for **1**–**5** (δ in ppm, J in Hz).

Position	1[a]	2[b]	3[c]	4[d]	5[e]
1a			1.84 (m)	2.62 (m)	1.98 (m)
1b			1.43 (m)	2.30 (m)	1.85 (m)
2a	2.77 (m)	2.76 (m)	1.77 (m)	2.45 (m)	1.94 (m)
2b	2.25 ddd (14.8, 8.1, 1.5)	2.24 ddd (14.8, 8.1, 1.5)	1.39 (m)	2.25 (m)	1.43 (m)
3	3.94 dt (11.0, 8.3)	3.90 dt (11.0, 8.3)	3.19 (m)	4.69 ddd (10.8, 8.4, 5.5)	3.49 (m)
5a	3.69 dd (15.4, 5.8)	3.50 dd (15.4, 5.8)	2.94 (m)	4.42 (m)	3.43 (m)
5b	3.44 dd (15.4, 11.3)	3.25 dd (15.4, 11.3)	2.94 (m)	4.33 (m)	3.10 dd (13.9, 12.0)
6a	1.75 (m)	1.84 (m)	1.66 (m)	2.14 (m)	1.80 (m)
6b	1.43 (m)	1.56 (m)	1.53 (m)	2.14 (m)	1.47 (m)
7a	1.99 (m)	1.95 (m)	1.66 (m)	1.96 (m)	1.68 (m)
7b	1.62 (m)	1.55 (m)	1.66 (m)	1.85 (m)	1.56 (m)
8a	1.89 (m)	1.73 (m)	3.57 (m)	2.36 (m)	1.94 (m)
8b	1.65 (m)	1.43 (m)		2.07 (m)	1.69 (m)
9	2.64 (m)	2.61 (m)			
9a			3.60 (m)	4.91 dd (12.1, 6.7)	3.49 (m)
10a	1.90 (m)	2.07 (m)	2.33 (m)	2.68 (m)	3.79 d (10.2)
10b	1.90 (m)	1.36 (m)	1.67 (m)	1.95 (m)	
11	2.36 (m)	2.19 (m)	2.75 (m)	3.00 (m)	2.57 (m)
13	1.03 d (7.0)	1.02 d (7.0)	1.13 d (7.0)	1.23 d (7.0)	1.21 d (7.0)
14	4.45 ddd (10.8, 8.4, 5.5)	4.45 ddd (10.8, 8.4, 5.5)	4.33 ddd (10.8, 8.4, 5.5)	5.11 ddd (10.8, 8.4, 5.5)	4.25 ddd (10.8, 8.4, 5.5)
15a	2.63 (m)	2.64 (m)	2.30 (m)	2.66 (m)	2.41 ddd (12.6, 8.4, 5.5)
15b	1.60 (m)	1.59 (m)	1.42 (m)	1.84 (m)	1.56 (m)
16	2.75 (m)	2.74 (m)	2.65 (m)	2.82 (m)	2.69 (m)
18	1.22 d (7.0)	1.21 d (7.0)	1.08 d (7.0)	1.18 d (7.0)	1.19 d (7.0)
OH			5.03 d (5.0)		

[a] 800 MHz in acetone $-d_6$.
[b] 600 MHz in acetone $-d_6$.
[c] 500 MHz in DMSO-d6.
[d] 500 MHz in acetone $-d_6$.
[e] 500 MHz in methanol-d_4.

Table 2
^{13}C NMR spectroscopic data for **1**–**5** (δ in ppm).

Position	1[a]	2[b]	3[c]	4[d]	5[e]
1	107.4 s	108.8 s	26.8 t	28.1 t	27.8 t
2	28.4 t	28.5 t	26.1 t	25.1 t	27.6 t
3	68.7 d	70.0 d	66.7 d	82.0 d	65.0 d
5	48.4 t	51.2 t	48.5 t	70.3 t	47.4 t
6	28.2 t	30.1 t	21.8 t	22.8 t	26.4 t
7	30.6 t	30.6 t	30.4 t	24.1 t	23.2 t
8	33.3 t	35.8 t	73.5 d	36.5 t	27.6 t
9	34.5 d	37.5 d	90.6 s	84.5 s	91.7 s
9a	172.6 s	172.9 s	62.9 d	92.1 d	72.2 d
10	39.9 t	41.5 t	33.8 t	43.4 t	80.0 d
11	36.1 d	39.7 d	35.0 d	34.4 d	41.6 d
12	192.0 s	192.7 s	179.3 s	177.9 s	178.1 s
13	16.3 q	15.9 q	17.0 q	15.9 q	12.5 q
14	81.5 d	81.7 d	80.3 d	74.0 d	84.6 d
15	34.3 t	34.0 t	34.1 t	35.1 t	35.4 t
16	35.1 d	35.2 d	34.2 d	34.8 d	36.0 d
17	179.2 s	179.3 s	179.4 s	178.3 s	182.2 s
18	15.0 q	15.1 q	14.5 q	14.7 q	15.0 q

[a] 200 MHz in acetone $-d_6$.
[b] 150 MHz in acetone $-d_6$.
[c] 125 MHz in DMSO-d6.
[d] 125 MHz in acetone $-d_6$.
[e] 125 MHz in methanol-d_4.

1 was an analogue of croomine-type alkaloids [4]. Further analysis of the NMR spectra indicated that **1** possessed an α-methyl-γ-lactone moiety (δ_C 179.2, 81.5, 35.1, 34.3 and 15.0) and an α,β-unsaturated carbonyl (δ_C 192.0, 172.6 and 107.4). Apart from four degrees of unsaturation accounted for by the above functionalities, the remaining three degrees of unsaturation suggested that **1** may have an unusual tricyclic core.

The planar structure of **1** was further constructed by 2D NMR spectroscopic analysis (Fig. 2, Tables 1 and 2). The structure of pyrrolo [1,2-*a*]azepine core (rings A and B) was established by the ^{1}H–^{1}H COSY correlations of H$_2$-2/H-3 and H$_2$-5/H$_2$-6/H$_2$-7/H$_2$-8/H-9, together with the HMBC correlations of H$_2$-2 (δ_H 2.77; 2.25, ddd, J = 14.8, 8.1, 1.5 Hz), H$_2$-5 (δ_H 3.69, dd, J = 15.4, 5.8 Hz; 3.44, dd, J = 15.4, 11.3 Hz) and H$_2$-8 (δ_H 1.89, 1.65) to C-9a (δ_C 172.6), and of H-3 (δ_H 3.94, dt, J = 11.0, 8.3 Hz) to C-5 (δ_C 48.4) and C-1 (δ_C 107.4). Meanwhile, ^{1}H–^{1}H COSY correlations of H-9/H$_2$-10/H-11/H$_3$-13 and HMBC correlations of H$_2$-10 (δ_H 1.90, 2H) to C-12 (δ_C 192.0) and C-9a (δ_C 172.6), and of H$_3$-13 (δ_H 1.03, d, J = 7.0 Hz) to C-12 indicated the existence of 6-methyl-cyclohex-2-enone ring system (ring C). HMBC cross-peaks of H$_2$-2 to C-12, C-1 and C-9a, and of H$_2$-10 to C-9a led to the connections of ring C to pyrrolo [1,2-*a*]azepine via C-1–C-9a–C-9. Thus, the unique tricyclic pyrrolo [3,2,1-*jk*]benzazepine-12-one core have been formed on the basis of the fragments established above.

In addition, the presence of the α-methyl-γ-lactone moiety (ring D) was also corroborated by ^{1}H–^{1}H COSY correlations of H-14/H$_2$-15/H-16/H$_3$-18 and HMBC correlations of H$_2$-15 (δ_H 2.63, 1.60), H-16 (δ_H 2.75) and H$_3$-18 (δ_H 1.22, d, J = 7.0 Hz) to C-17 (δ_C 179.2). Connection of rings D and A via C-3 (δ_C 68.7) was elucidated by ^{1}H–^{1}H COSY correlation of H-3/H-14 and HMBC correlation of H$_2$-2 to C-14 (δ_C 81.5). Thereby, the planar structure of **1** was established as depicted.

The relative configuration of **1** was deduced from the analysis of its ROESY spectra in combination with its biogenetic consideration (Fig. 3). The ROESY correlation of H-14/H-16 indicated that both protons were cofacial and were arbitrarily assigned as β-oriented [2]. The correlations of H-3/H-15b, and H-15b/CH$_3$-18 established the α-orientation of H-3. Meanwhile, the correlations of H-9/H-5b and H-3/H-5a, and the absence correlation of H-9/H-11 revealed that H-9 and CH$_3$-13 were all β-oriented. Therefore, the relative configurations of **1** was assigned as 3*S**, 9*R**, 11*R**, 14*S**, and 16*S**.

Stemtuberline B (**2**) was obtained as a white solid, and was assigned the molecular formula $C_{18}H_{25}NO_3$ based on HRESIMS *m/z* 326.1724 [M + Na]$^+$ (calcd for 326.1727). Compounds **2** and **1** possessed the same molecular formula, and the 1D NMR spectra of **2** indicated both compounds shared the same skeleton. The striking differences were the chemical shifts of at C-8, C-9, C-10 and C-11 position were downfield shifted $\Delta\delta_C$ +2.5, +3.0, +1.6 and + 3.6 ppm in **2**, respectively, which indicated that **2** might be epimer of **1** at C-9 position. The assignment could also resulted in the upfield shift of H-11 (δ_H 2.19, $\Delta\delta_H$ −0.17) by the γ-steric compression effect from H-9 to H-11. Furthermore, the key ROESY correlation of H-9/H-11 revealed that H-9 took the same orientation with that of H-11 and thus established the relative configuration of **2**. The other parts were identical with **1** which was confirmed by detailed 2D NMR (^{1}H–^{1}H COSY, HMBC and ROESY) spectra. Accordingly, the structure of **2** was assigned as shown (Fig. 1).

The absolute configurations of **1** and **2** were determined by time-dependent density functional theory electronic circular dichroism (TDDFT ECD) calculations [5]. A comparison between the experimental and calculated ECD spectra using the DFT (density functional theory) method at the B3LYP/6-311G* level was performed. The measured ECD spectra exhibited an excellent fit with the calculated ECD spectra (Fig. 4 and Fig. 5). Therefore, the absolute configurations of the stereogenic centers of **1** and **2** were assigned as 3*S*, 9*R*, 11*R*, 14*S*, 16*S* and 3*S*, 9*S*, 11*R*, 14*S*, 16*S*, respectively (Fig. 1).

A plausible biosynthetic pathway for the formation of **1** and **2** was proposed in Scheme 1. The biogenetic precursor of them might be originated from the coexistence alkaloid croomine (**6**). **6** underwent hydrolysis and subsequent dehydration to obtain intermediates A and B, and then the rearrangement of intermediate B afforded important intermediate C. The intramolecular nucleophilic addition-elimination of intermediate C could produce

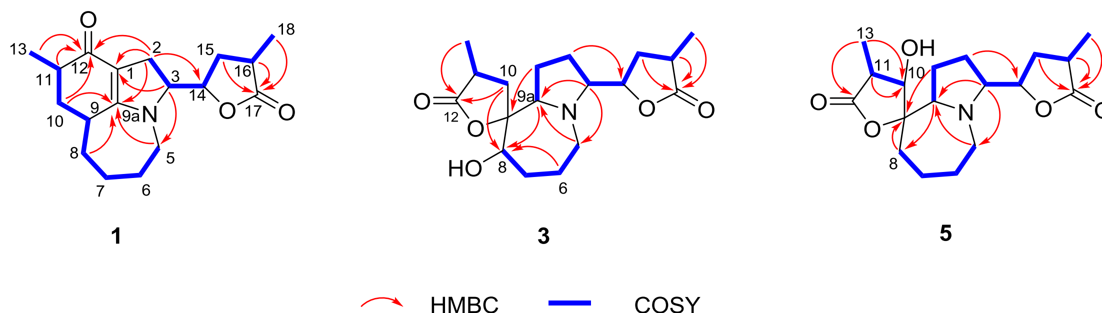

Fig. 2. Key HMBC and ^{1}H–^{1}H COSY correlations of compounds **1**, **3**, and **5**.

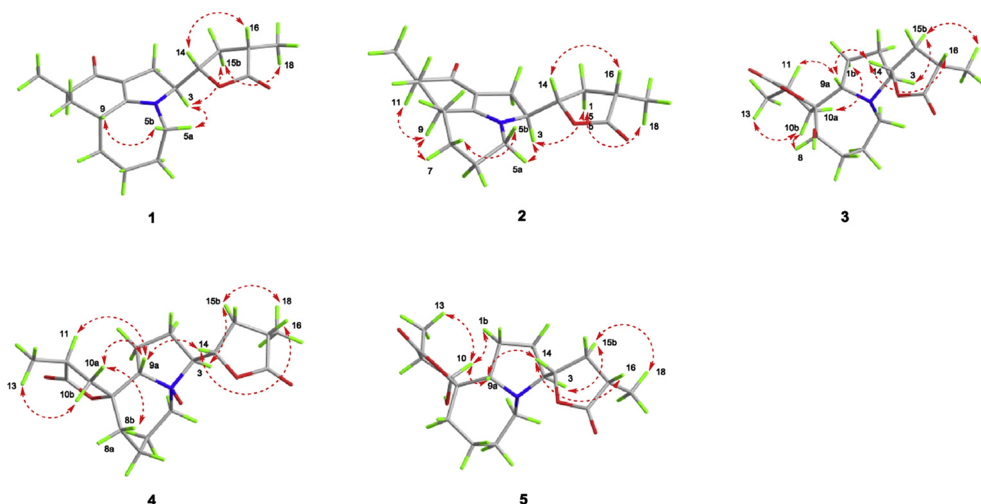

Fig. 3. Key ROESY correlations of compounds **1**–**5**.

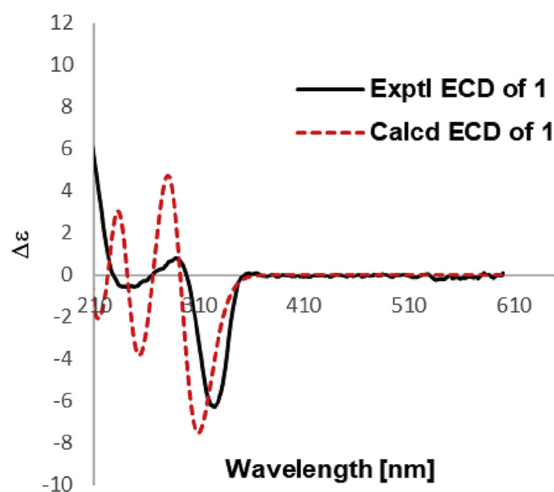

Fig. 4. Calculated and experimental ECD spectra of **1**.

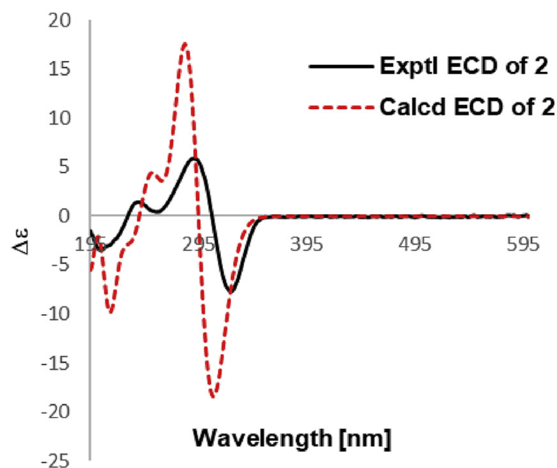

Fig. 5. Calculated and experimental ECD spectra of **2**.

intermediate D, which were finally converted to compounds **1** and **2** by the subsequent intramolecular rearrangement, respectively.

Stemtuberline C (**3**), was obtained as yellow amorphous solid, and its molecular formula was assigned as $C_{18}H_{27}NO_5$, with six degrees of unsaturation, from its HRESIMS (*m*/*z* 336.1818 $[M - H]^-$, calcd for 336.1816) and NMR data (Tables 1 and 2). The IR absorptions at 1772 cm^{-1} and 3438 cm^{-1} indicated the existence of an ester carbonyl and a hydroxyl group, respectively. The ^1H and ^{13}C NMR data suggested that compound **3** contained a basic croomine-type skeleton and had a great similarity with that of croomine [6]. The presence of a methine resonanced at δ_C 73.5 in **3** indicated that **3** was hydroxyl analogue of croomine. HMBC correlations of H_2-6 (δ_H 1.66, 1.53), H-9a (δ_H 3.60) and H_2-10 (δ_H 2.33, 1.67) to C-8 (δ_C 73.5) demonstrated that compound **3** was the 8-hydroxyl derivative of croomine (Fig. 2). The relative configuration of **3** was identical to that of croomine [6]. Meanwhile, the ROESY correlations of H-8/H-10b, and H-10b/CH_3-13 indicated that H-8 was α-oriented. Accordingly, the relative configuration of **3** was established as 3*S**, 8*R**, 9*S**, 9a*S**, 11*R**, 14*S**, and 16*S**.

Stemtuberline D (**4**) was obtained as a yellow amorphous powder. The HRESIMS suggested the molecular formula was $C_{18}H_{27}NO_5$ (*m*/*z* 338.1961 $[M + H]^+$; calc for 338.1962). The strong and sharp IR band at 1781 cm^{-1} indicated the existence of an ester carbonyl. The ^{13}C NMR spectrum of **4** (Table 2), in combination with the DEPT spectrum, revealed the presence of two methyls, eight methylenes, five methines, and three quaternary carbons. Further analysis of the HSQC, $^1H-^1H$ COSY and HMBC spectra found that compound **4** was highly similar to croomine (**6**) [6], while the significant differences were the signals at C-3 (δ_C 68.3), C-5 (δ_C 50.0), and C-9a (δ_C 70.6) in croomine were downfield shifted $\Delta\delta_C$ +13.7, +20.3, and +21.5 ppm in **4**, respectively. Furthermore, the molecular weight of compound **4** is 16 mass units larger than that of croomine, indicated that compound **4** was the *N*-oxide form of croomine.

The ROESY spectrum of **4** was generally similar to that of croomine [6], the major difference was the observation of the correlation of H-10a/H-8b (Fig. 3). Namely, C-9 in compound **4** was determined to be *R** configuration. The relative configuration of **4** was thus established as 3*S**, 9*R**, 9a*S**, 11*R**, 14*S**, and 16*S**.

Stemtuberline E (**5**) was isolated as a white amorphous powder, and was assigned to have a molecular formula of $C_{18}H_{27}NO_5$ based on HRESIMS *m*/*z* 338.1962 $[M + H]^+$ (calcd for 338.1962). The IR absorptions at 1773 cm^{-1} and 3431 cm^{-1} indicated the existence of an ester carbonyl and a hydroxyl group, respectively. The ^{13}C NMR spectrum of **5** (Table 2), in combination with the DEPT spectrum,

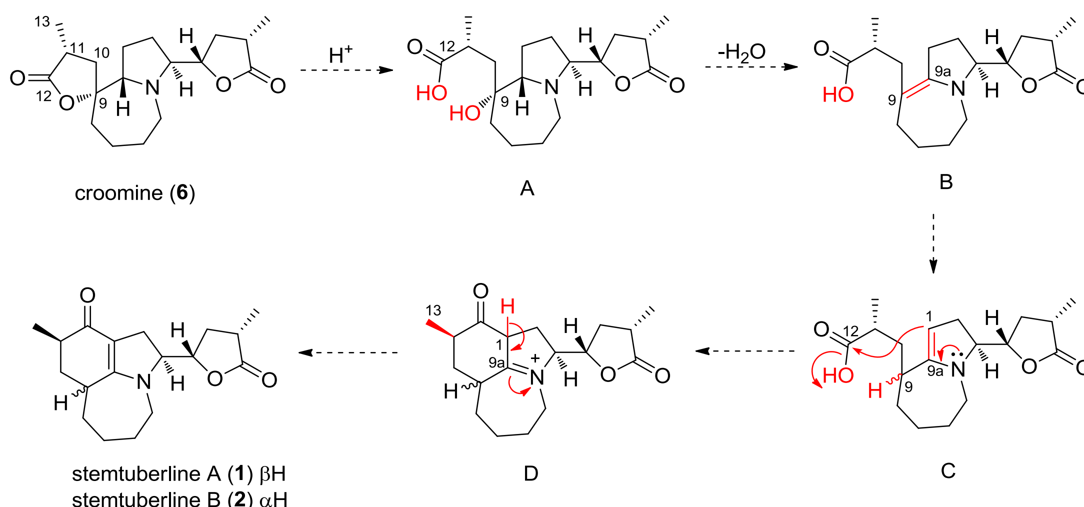

Scheme 1. Plausible biosynthetic pathway for compounds **1** and **2**.

revealed the presence of two methyls, seven methylenes, six methines, and three quaternary carbons. Detailed analysis of the NMR data (Tables 1 and 2) indicated **5** shared the same planar structure with that of 10-hydroxycroomine [7]. The observation of the downfield shifts of C-13 ($\Delta\delta_C$ +2.5) and C-10 ($\Delta\delta_C$ +7.6) in **5** suggested that **5** was the epimer of 10-hydroxycroomine, which thus resulted in the upfield shift of H-13 ($\Delta\delta_H$ −0.06) in **5** due to the γ-steric compression effect. Furthermore, the key ROESY correlation of H-10/CH_3-13 confirmed the above elucidation.

Seven known compounds (**6**–**12**) were respectively identified as croomine (**6**) [6], 6-hydroxycroomine (**7**) [8], stemotinine (**8**) [9], didehydrocroomine (**9**) [6], dehydrocroomine (**10**) [7], dehydroisostemotinine (**11**) [10], and tuberostemospiroline (**12**) [11], by comparison of their spectroscopic data with those literature.

The *anti*-TMV activity of the isolates was tested in *Nicotiana glutinosa* using the half-leaf method [12]. The results showed that compound **11** exhibited the best activity at concentration of 50 μg/mL, with the curative inhibition rate was 84.6%, higher than that of ningnamycin (52.9%).

3. Conclusions

In this investigation, two novel stemona alkaloids (**1**–**2**), three new croomine-type alkaloids (**3**–**5**) and seven known substances (**6**–**12**) were isolated from the roots of *S. tuberosa*. Alkaloids **1** and **2** are a pair of epimers and featured a unique tricyclic pyrrolo [3,2,1-*jk*]benzazepine-12-one nucleus. Their *anti*-TMV activities were firstly evaluated, compound **11** exhibited the significant *anti*-TMV activity at concentration of 50 μg/mL, with the curative inhibition rate were 84.6%.

4. Experimental

4.1. General experimental procedures

NMR spectra were measured via a Bruker AV-500 MHz, or a Bruker Avance III 600 MHz, or a Bruker AV-800 MHz spectrometer, TMS was used as an internal standard. Optical rotations were recorded on a Horiba SEPA-300 polarimeter. ECD spectra were acquired with a Chirascan instrument. UV spectra were collected on a Shimadzu UV-2401PC spectrometer. ESIMS and HRESIMS were obtained on an API QSTAR Pulsar 1 spectrometer. Column chromatography (CC) was performed on either C-18 silica gel (40–60 μm; Daiso Co., Japan), MCI gel CHP 20P (75–150 μm, Mitsubishi Chemical Industries, Tokyo, Japan), silica gel (300–400 mesh; Qingdao Marine Chemical Inc., P. R. China) or Sephadex LH-20 (Amersham Pharmacia, Sweden). Semi-preparative HPLC was carried out using an Agilent 1100 liquid chromatograph equipped with a Phenomene Luna 5μ C18 (2) 100A column (250 mm × 10 mm, 5 μm).

4.2. Plant material

The roots of *S. tuberosa* used in this investigation were purchased from Kunming Luosiwan Chinese medicine market, in Jul 2017. The plant species was authenticated by Prof. Hua Peng, and the voucher specimen (KIB20170716) was deposited in the State Key Laboratory of Phytochemistry and Plant Resources in West China, Kunming Institute of Botany, Chinese Academy of Science (CAS).

4.3. Extraction and isolation

Dried and powdered *S. tuberosa* (40 kg) was extracted with MeOH under condition reflux to give a crude extract, which was suspended in 3% HCl followed by extraction with petroleum ether. The acidic aqueous extract was basified (pH 9–10) with 25% aqueous NH_4OH, and then extracted with CH_2Cl_2, and evaporated the solvent under reduced pressure to afford a crude alkaloid extract (100 g). The crude alkaloid was further divided into four parts (Fr. A-D) by RP-18 column eluting with MeOH/H_2O (10:90 to 100:0). Fr. A (2 g) was purified on a silica gel column, and eluted with CH_2Cl_2/MeOH (200:1 to 40:1) to afford compounds **6** (0.4 g), **7** (0.24 g) and **9** (45 mg). Fr. B (15 g) was subsequently fractionated by RP-18 column eluting with MeOH/H_2O (30:70 to 100: 0) gradient to provide four portions (Fr.B.1–4). Of these, Fr.B.1 (2.3 g) was subjected to Sephadex LH-20 (MeOH), followed by a silica gel (CH_2Cl_2/MeOH, 100:1) to yield compounds **8** (42 mg) and **10** (11 mg). Fr.B.2 (2.5 g) was separated via semipreparative HPLC using MeCN–H_2O (35:65) as the mobile phase to afford compounds **1** (1.2 mg, t_R = 12.0 min), **2** (1.7 mg, t_R = 15.0 min) and **11** (10.8 mg, t_R = 20 min). Fr. C (12 g) was loaded onto a silica gel column and eluted with petroleum/acetone/Et_2NH (50:1:0.1 to 1:1:0.1) to furnish three portions (Fr.C.1–3). Fr.C.2 (4.3 g) was separated by Sephadex LH-20 (MeOH), followed by a silica gel (CH_2Cl_2/MeOH, 200:1 to 40:1) to afford compounds **3** (18 mg), **4** (45 mg) and **12**

(180 mg). Fr.C.3 (1.2 g) was subjected to Sephadex LH-20 (MeOH), followed by semi-preparative HPLC ($MeOH/H_2O$, 40:60, V/V) to yield compound **5** (28 mg, $t_R = 18.0$ min).

4.4. Compound characterization data

*Stemtuberline A (**1**):* white solid; [α]20 D −38.8 (*c* 0.07, CH_3OH); UV (CH_3OH) λ_{max} (log ε): 250 (3.17), 323 (4.15) nm; ECD (0.0007 M, CH_3OH) λ_{max} ($\Delta\varepsilon$) 198 (+3.54), 325 (−2.7); IR (KBr) v_{max} 3440, 2935, 1768, 1717, 1642, 1457, 1198, 1173 cm^{-1}; ^1H and ^{13}C NMR data (acetone−d_6, 800 and 200 MHz) see Tables 1 and 2; HRESIMS *m/z* 326.1724 $[M + Na]^+$ (calcd for $C_{18}H_{25}NO_3Na$, 326.1727).

*Stemtuberline B (**2**):* white solid; [α]20 D −30.8 (*c* 0.12, CH_3OH); UV (CH_3OH) λ_{max} (log ε): 263 (3.13), 323 (4.17) nm; ECD (0.00087 M, CH_3OH) λ_{max} ($\Delta\varepsilon$) 204 (−1.2), 289 (+2.1), 325 (−2.7); IR (KBr) v_{max} 3435, 2938, 1774, 1712, 1647, 1458, 1192, 1166, 1024 cm^{-1}; ^1H and ^{13}C NMR data (acetone−d_6, 600 and 150 MHz) see Tables 1 and 2; HRESIMS *m/z* 326.1724 $[M + Na]^+$ (calcd for $C_{18}H_{25}NO_3Na$, 326.1727).

Stemtuberline C (**3**): yellow amorphous solid; [α]20 D −4.3 (*c* 0.35, CH_3OH); IR (KBr) v_{max} 3438, 2936, 1772, 1678, 1456, 1168, 1164, 1021, 925 cm^{-1}; ^1H and ^{13}C NMR data (DMSO-d6, 500 and 125 MHz) see Tables 1 and 2; HRESIMS *m/z* 336.1818 $[M - H]^-$ (calcd for $C_{18}H_{26}NO_5$, 336.1816).

*Stemtuberline D (**4**):* yellow amorphous powder; [α]20 D 2.6 (*c* 0.22, CH_3OH); IR (KBr) v_{max} 3439, 2942, 1781, 1682, 1200, 1135, 1024 cm^{-1}; ^1H and ^{13}C NMR data (acetone−d_6, 500 and 125 MHz) see Tables 1 and 2; HRESIMS *m/z* 338.1961 $[M + H]^+$ (calcd for $C_{18}H_{28}NO_5$, 338.1962).

Stemtuberline E (**5**): white amorphous powder; [α]20 D −19.2 (*c* 0.15, CH_3OH); IR (KBr) v_{max} 3431, 2938, 1773, 1732, 1667, 1455, 1196, 1170, 1027 cm^{-1}; ^1H and ^{13}C NMR data (methanol-d_4, 500 and 125 MHz) see Tables 1 and 2; HRESIMS *m/z* 338.1962 $[M + H]^+$ (calcd for $C_{18}H_{28}NO_5$, 338.1962).

4.5. Anti-TMV activity assay

4.5.1. Protective effect in vivo

The compound solutions were smeared on the left side of the leaves of *N. glutinosa*, whereas the DMSO solvent was smeared onto the right side of the same leaf as a negative control. After 6 h, 100 μL of TMV particles (50 µg/mL) were inoculated onto each half of the leaf, respectively. Each inoculated leaf was washed with water after 10 min, and the numbers of local lesions were recorded 3 or 4 days after inoculation. Three replicates were conducted for each compound and control agent [12].

4.5.2. Curative effect in vivo

TMV particles (50 µg/mL) were inoculated onto whole leaves of *N. glutinosa*. After 24 h, the compound solutions were smeared onto the left half of TMV-inoculated leaf, while the DMSO solution was smeared onto the right side as a negative control. The local lesion numbers were recorded 3 or 4 days after inoculation. Three repetitions were conducted for each compound [12].

Acknowledgements

This research was supported financially by grants from the National Science Foundation of China (21432010), Technological leading talent project of Yunnan (2015HA020), CAS “Light of West China” Program (to Y. Z.), the Youth Innovation Promotion Association of CAS (2015323), the Young Academic and Technical Leader Raising Foundation of Yunnan Province (to Y. Z.), and the Natural Science Foundation of Guizhou (QKHLH-2015-7405).

Appendix A. Supplementary data

Supplementary data to this article can be found online at https://doi.org/10.1016/j.tet.2018.11.064.

References

[1] (a) R.A. Ramli, W. Lie, S.G. Pyne, Tetrahedron 53 (2008) 491–4944;
(b) S. Kongkiatpaiboon, J. Schinnerl, S. Felsinger, V. Keeratinijakal, S. Vajrodaya, W. Gritsanapan, L. Brecker, H. Greger, J. Nat. Prod. 74 (2011) 1931–1938.
[2] (a) R.A. Pilli, M.C. Ferreira de Oliveira, Nat. Prod. Rep. 17 (2000) 117–127;
(b) F.-P. Wang, Q.-H. Che, Nat. Prod. Commun. 9 (2014) 1809–1822;
(c) Y. Hitotsuyanagi, Y. Sekiya, H. Fukaya, H.S. Park, S. Zhu, K. Komatsu, Tetrahedron Lett. 57 (2016) 5746–5749;
(d) S.-Z. Huang, F.-D. Kong, Q.-Y. Ma, Z.-K. Guo, L.-M. Zhou, Q. Wang, H.-F. Dai, Y.-X. Zhao, J. Nat. Prod. 79 (2016) 2599–2605.
[3] (a) E. Kaltenegger, B. Brem, K. Mereiter, H. Kalchhauser, H. Kählig, O. Hofer, S. Vajrodaya, H. Greger, Phytochemistry 63 (2003) 803–816;
(b) Y. Wu, L.T. Ou, D. Han, Y.B. Tong, M. Zhang, X.H. Xu, C.F. Zhang, Fitoterapia 112 (2016) 22–29.
[4] (a) P. Pudjiastuti, S.G. Pyne, Sugiyanto, W. Lie, Phytochem. Lett. 5 (2012) 358–360;
(b) Y. Yue, A.-J. Deng, D.-S. Xu, H.-L. Qin, J. Asian Nat. Prod. Res. 15 (2013) 145–150.
[5] (a) H. Gotō, E. Ōsawa, J. Chem. Soc., Perkin Trans. 2 (1993) 187–198;
(b) H. Gotō, E. Ōsawa, J. Am. Chem. Soc. 111 (1989) 8950–8951.
[6] T. Noro, S. Fukushima, A. Ueno, T. Miyase, Y. Iitaka, Y. Saiki, Chem. Pharm. Bull. 27 (1979) 1495–1497.
[7] L.-G. Lin, H.P. Leung, J.-Y. Zhu, C.-P. Tang, C.-Q. Ke, J.A. Rudd, G. Lin, Y. Ye, Tetrahedron 64 (2008) 10155–10161.
[8] R.-W. Jiang, P.-M. Hon, Y.-T. Xu, Y.-M. Chan, H.-X. Xu, P.-C. Shaw, P. Pui-Hay But, Phytochemistry 67 (2006) 52–57.
[9] R.-S. Xu, Y.-J. Lu, J.-H. Chu, Tetrahedron 38 (1982) 2667–2670.
[10] J. Guo, H.-P. He, S.-L. Li, H.-M. Hua, X.-J. Hao, Acta Bot. Yunnanica 32 (2010) 463–465.
[11] J.-P. Hu, D.-H. Yang, W.-H. Lin, S.-Q. Cai, Helv. Chim. Acta 92 (2009) 2125–2133.
[12] (a) L. Zhao, J. Dong, Z. Hu, S. Li, X. Su, J. Zhang, Y. Yin, T. Xu, Z. Zhang, H. Chen, Pestic. Biochem. Phys. 140 (2017) 24–29;
(b) Q.-F. Hu, B. Zhou, X.-M. Gao, L.-Y. Yang, L.-D. Shu, Y.-Q. Shen, G.-P. Li, C.-T. Che, G.-Y. Yang, J. Nat. Prod. 75 (2012) 1909–1914.